THERMAL DESIGN OF FUTURE MEDIUM VOLTAGE SWITCHGEAR

Elin FJELD
Telemark University College – Norway
elin.fjeld@hit.no

Wilhelm RONDEEL
TUC – Norway
wilhelm.rondeel@hit.no

Knut VAAGSAETHER
TUC - Norway
knut.vagsater@hit.no

Magne SAXEGAARD
ABB – Norway
magne.saxegaard@no.abb.com

Pål SKRYTEN
ABB – Norway
pal.skryten@no.abb.com

Elham ATTAR
ABB - Norway
elham.attar@no.abb.com

ABSTRACT

Air is a desirable alternative to SF_6 in medium voltage (MV) switchgear. However, the thermal properties of air is poorer compared with SF_6, and this paper presents a first step in the process of finding an optimized thermal design. Mapping of the resistances and the thermal condition have been performed on a custom made prototype. Together with CFD-simulations, these methods are found to be useful for gaining insight and improving the thermal design of MV switchgear. The combined contact resistances (bolted and others) was for found to constitute about 35 % of the total resistance of the prototype. Possible contributions from the skin-effect and/or iron losses seem to be of little or no influence to the power input.

INTRODUCTION

Medium voltage (MV) switchgears are used in the distribution network to ensure a safe and reliable power supply to the customers. For decades, SF_6 gas has been used to ensure the reliability, compactness, and robustness of these switchgears. Unfortunately, SF_6 suffers from a very high global warming potential. MV switchgears are manufactured to be sealed for life and to have SF_6 emissions of < 0.1 % / year. Nevertheless, since SF_6 emission can occur due to incorrect handling during installation and decommissioning, the industry is interested in finding a suitable alternative.

For the future generation of MV switchgears, it is desirable to keep the compact switchgear design [1]. Load currents cause ohmic losses and thus heating inside the switchgear. Air is a desirable alternative to SF_6, however, since the thermal properties of air is poorer compared with SF_6, this causes some extra care to be taken regarding the thermal design in order to satisfy the requirements of the temperature rise test specified in the standard IEC 62271-1 [2].

Thermal design has traditionally been devoted little attention as SF_6 has relatively good thermal properties. To be able to keep the compact design when changing to a more environmental friendly gas, thermal design needs to be more optimized. This paper presents the results from the first step in this process. Mapping of the resistances and the thermal condition have been performed on an air filled prototype with dimensions comparable to an SF_6-filled switchgear installation. The temperature and power measurements are used as input data in simplified heat transfer simulations. ANSYS-fluent CFD software is used in addition to calculations according to the empirical guidelines given in IEC TR 60890 [3].

TEST OBJECT

The experiments described in this paper were performed on a (non-commercial) 12 kV custom made prototype, made for the purpose of testing and verification of models and simulations. The unit consisted of three modules, as can be seen in Figure 1, with total dimensions corresponding to SF_6-filled 12/24 kV switchgear. Two of the modules (C1 and C3 in Figure 1) were equipped with load break cable switches (LBS) of a puffer type enclosed in a closed plastic cylinder. The center module of the test object (V2 in Figure 1) was the transformer T-off which was equipped with a vacuum circuit breaker (VCB). The switchgear was filled with air at atmospheric pressure. Commercial switchgear is typically filled with an overpressure and has thus somewhat better thermal properties.

Figure 1: Front view of the test object with two cable modules (C1 and C3) with LBS and a transformer T-off (V2) with a vacuum circuit breaker.

All the conductors were made of bare or silver coated copper (Cu), except the busbars which were made of silver coated aluminum (Al). Relevant material properties are given in Table 1. The different conductor pieces are connected by bolted connections. In addition, there are an open/close contact and a sliding contact inside the LBS housing.

Table 1: Material properties [4]. ρ is the specific resistance and α is the temperature coefficient of typical alloys of the given material.

Conductor material	ρ [$\Omega mm^2/m$]	α [1/K]
Cu	0.0179	0.0039
Al	0.032	0.0036

EXPERIMENTAL PROCEDURE

Thermal testing were carried out at the 630 A rated three-phase current, at a frequency of 50 Hz, supplied from a high current injector test equipment, Hilkar Elektroteknik Ltd, type AK23. The vacuum module (center module) was electrically disconnected, and the current was passing from one cable module via the busbars through the second cable module. That means that the current was passing through two LBS for each phase, as can be seen in Figure 2. This is the normal path for the main current through the switchgear during normal conditions in a common cable ring distribution system. The heat dissipated in the enclosed switchgear will be generated along this current path. There are ten bolted connections along the current path, as shown in Figure 2. In addition, each of the LBS contained two bolted connections, an open/close contact and a sliding contact.

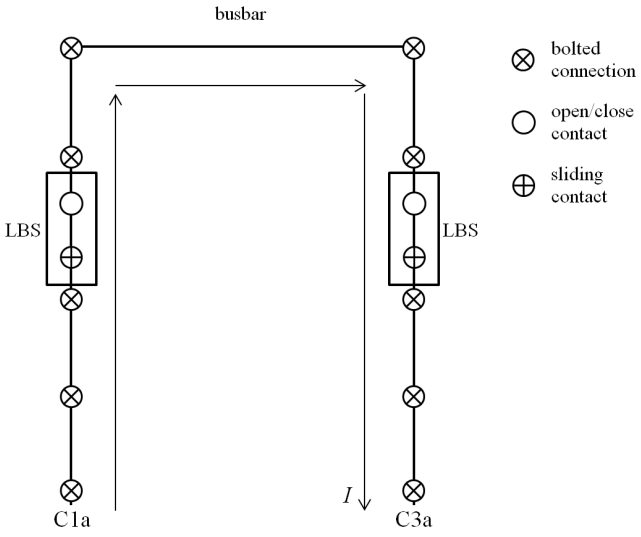

Figure 2: The current path for one of the three phases of the switchgear in Figure 1. The current (I) was passing through one cable module, via the busbar, and through the next cable module.

Thermocouples were connected to the conductors along the current path, and the temperature just above the LBS was monitored during heating until steady state conditions were reached (temperature increase less than 1 ˚C pr. hour). The temperature along the current path, the air temperature inside the switchgear, and the power dissipated were measured at steady state conditions. Then the AC supply was disconnected and a DC source of 100 A was connected for resistance measurements along the current path.

TEMPERATURE MEASUREMENTS

A number of thermocouples (20) of type K were mounted on both sides of every contact pair along the current path for each phase. After the equipment was heated to steady state, the temperature of each point was measured, and the results are shown in Figure 3. The average temperature rise along the current path was found to be 74 ˚C. The highest temperature increase was measured inside the LBS.

The steady state temperature rise in all of the components should be within the permissible limits, as specified by the standard IEC 62271-1, for the switchgear to be able to pass a temperature rise test. The limit is 75 ˚C for bolted connections (where at least one side is silver- or nickel coated) and 65 ˚C for open/close contacts and sliding contacts (silver- or nickel coated). These upper limits are indicated in Figure 3 by a dotted and a solid horizontal line, respectively. From the figure it is clear that the measured values outside and inside the LBS are higher than acceptable.

The temperatures at all the contacts are expected to be higher than what is measured some short distance away. The open/close and sliding contacts are located inside a closed plastic housing. Measurements performed on the main conductor inside the LBS gave a temperature 1-2 degrees higher compared to the outside.

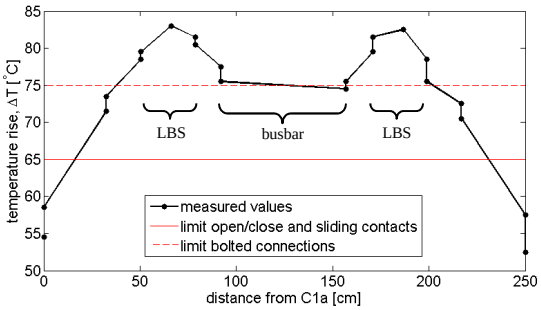

Figure 3: Measured temperature rise (ΔT) as a function of the distance from point C1a (ref. Figure 2), i.e. along the current path. The temperature limits specified by IEC 62271-1 are indicated by the horizontal lines.

The measured air temperatures are given in the first row of Table 2. The measurement of the air temperature at the top of the enclosure (ΔT_{top}) was performed 1 cm below the top surface.

Table 2: Temperature of the ambient air (T_{amb}), and temperature rise at the vertical mid-point inside the enclosure (ΔT_{mid}) and close to the top of the enclosure (ΔT_{top}) at steady state.

	T_{amb} [°C]	ΔT_{mid} [°C]	ΔT_{top} [°C]
Measured	18	37	47
IEC calculation	-	35	44
CFD simulation	-	40	55

MAPPING OF RESISTANCES

Resistance measurements at ambient, no-load ("cold") conditions were made before measurements at load currents ("warm" conditions). After the temperature measurements were made at steady state with rated current, the AC current source was disconnected and a 100 A DC source connected immediately afterwards. Measurements of the voltage drops along the current path were made within a few minutes, before the temperature dropped more than 10 %. From these measurements the resistances at "warm" conditions (R) were determined. The connection points were at the same locations as the temperature measurements were taken (the thermocouple wire was used as a connection to the outside of the compartment).

The accumulated resistance for phase 1 is plotted in Figure 4 for both "cold" and "warm" conditions. Table 3 gives the total resistance from C1a to C3a (c.f. Figure 2) for each phase. The measurements were performed between the inside bushing connection points.

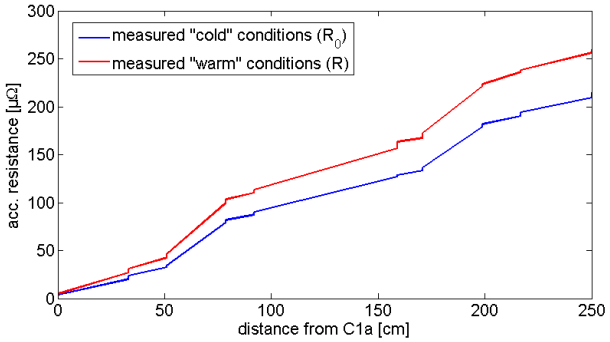

Figure 4: Accumulated resistance along the current path for phase L1.

Table 3: Resistance (based on measured voltage drop) for all phases during both "cold" (R_0) and "warm" (R) conditions. The measurements were performed from/to the inside bushing connection points.

	R_0 [µΩ]	R [µΩ]
Total phase L1	215	260
Total phase L2	203	241
Total phase L3	221	260

By summing the contact resistances and the bulk resistances separately, it may be concluded that the combined contact resistances (bolted and others) constitutes about 35 % of the total resistance at "cold" conditions.

An average value for the resistance of the bolted connections was calculated to be 4.0 µΩ based on measured values during "cold" conditions. This is in the same range as values reported in [5].

The bulk resistance at "cold" conditions is in agreement with theoretical calculations based on conductor lengths, cross-sectional area and specific resistance given in Table 1. The expected increase in bulk resistance with temperature can be calculated by [6]

$$R = R_0 \cdot (1+\alpha(T-T_0)) \quad (1)$$

where R is the resistance at temperature T, R_0 is the reference resistance at temperature T_0, and α is the temperature coefficient at T_0. The measured increase in bulk resistance is found to be as expected based on equation (1) with the temperature measurements, the resistance measured during "cold" conditions (R_0) and the temperature coefficients for the relevant materials in Table 1. It seems the increase from "cold" to "warm" conditions is higher for the contact resistance than the bulk resistance. This is as expected since the temperature increase in the contacts is even higher than for the bulk.

The resistance was measured across the total LBS. In addition, a measuring point was located at the main contact inside the LBS, i.e. between the open/close and the sliding contact. The measurements showed that the resistance of the part of the LBS containing the sliding contact was about twice the part containing the open/close contact (including other connections).

POWER MEASUREMENTS

The resistances of the conductors and the connections between the separate conductors are the main heat sources to the system. The measured values are however made with a DC source, and additional losses may be expected when operating at AC supply due to a possible skin effect. In addition, losses may occur in magnetic

steel surrounding the current path due to Eddy-currents and hysteresis losses. The latter may eventually be eliminated by using nonmagnetic materials, but with some possible cost consequences.

To investigate a possible contribution from these additional effects, the power dissipated in the switchgear was measured directly with a Gossen Metrahit Energy M249A wattmeter. The measurements were performed on the outside bushing connection point, and a total power loss of 350 W was found.

The ohmic heat loss based on the resistance measurements are

$$P_{ohm} = R_{tot} I^2 \quad (2)$$

where R_{tot} is the sum of the measured resistances for all three phases at rated current. Using the values given in Table 3 and adding the resistance across the bushings, gives a value of 348 W. Based on this, any contributions from skin-effect and induced currents in the enclosure seems to be insignificant. This is in contrast to Dong et al. [7] who found a skin-effect factor of 1.508 for a GIS with a rated current of 2500 A. This suggests that any possible influence of the skin-effect depends strongly on the current and the conductor design.

IEC CALCULATIONS

The IEC TR 60890 [3] provides a method to calculate the temperature rise of the air inside the enclosure by empirical data found by tests on other assemblies.

The effective surface area of the enclosure in Figure 1 was found to be 2.21 m^2. The installation was considered to be a separate enclosure, detached on all sides, without ventilation openings, zero internal horizontal partitions, and covered top and side surfaces. The input power loss was set to 326 W based on the measured resistances along the current path plus half of the resistance across each bushing.

The calculated temperature rises at the vertical mid-point of the enclosure and close to the top was found to be 35 ˚C and 44 ˚C, respectively. This is 2-3 ˚C lower than the measured temperature rises given in Table 2.

CFD SIMULATIONS

CFD-simulations was used to identify high temperature regions and areas with low heat transfer (low velocities). The simulations were carried out by the ANSYS-Fluent software. The fluid was modeled as incompressible ideal gas which takes into account density variations in the air due to changing temperature. No turbulence model was used since the flow velocities are low inside the compartment. The connectors and switches that act as heat sources were modeled as constant temperature sources where the measured surface temperature (Figure 3) was used. An assumption of flat plate free convection was used to model the heat transfer from the outside wall surface to the surrounding air.

Figure 5 shows the simulation domain with some outer walls removed. Figure 6 shows the simulated temperature field inside the compartment at a center plane. The large component close to the top is the bus bar. The temperature increase at the vertical mid-point of the enclosure and close to the top was found to be 40 ˚C and 55 ˚C, respectively, which is somewhat higher than the measured temperatures in Table 2.

Figure 7 shows the simulated velocity field in the same plane as in Figure 6. Even if the simulated velocity field shows local higher velocity the temperature shows a clear layering where the higher temperature air is collected at the top of the compartment. Higher heat transfer rates from the air to the wall can be achieved by increasing velocities along the wall.

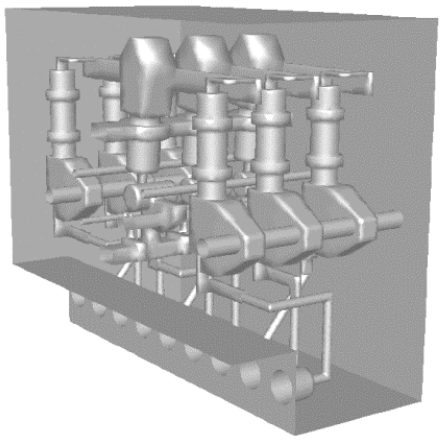

Figure 5: Switchgear simulation domain.

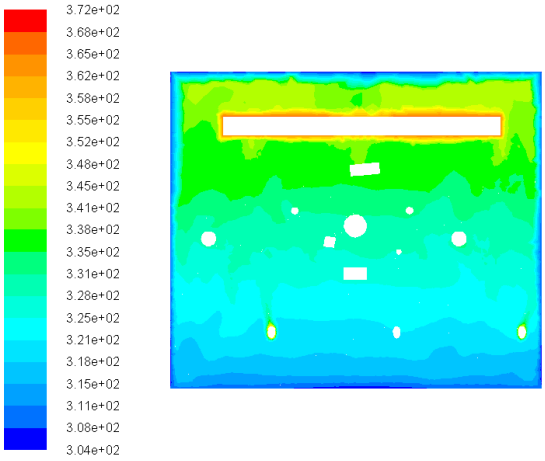

Figure 6: Simulated temperature field [K] inside the compartment. Image shown is a cut-plane in the center of the compartment where the structure in the top part is the busbar.

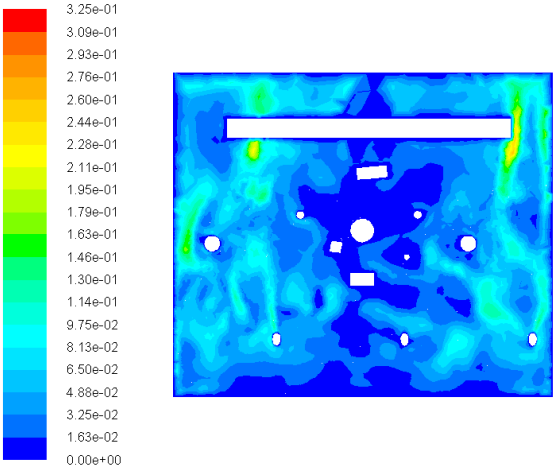

Figure 7: Simulated velocity field [m/s] inside the compartment. Image shown is a cut-plane in the center of the compartment.

CONCLUSIONS

The hottest spots were located inside the LBS. The prototype (custom made for the purpose of testing and verification of models and simulations) would not have passed the temperature rise test criteria given by the international standard IEC 62271-1 as measured temperatures up to 18 ˚C above the acceptable limits. The contact resistance was found to constitute approximately 35 % of the total resistance in the switchgear under test.

Power measurements showed that contributions from the skin effect and induced currents in the steel compartment are most probably insignificant in the prototype test switchgear at 630 A.

Calculations performed based on the empirical guidelines given in IEC TR 60890 gave air temperatures inside the switchgear only 2-3 ˚C lower than measured.

A simple CFD-model has been developed. The model gave realistic temperatures and velocity profiles which can be used to optimize the heat transport.

The resistance mapping, temperature measurements, resistance models and thermal modelling (CFD) performed in this study are found to be useful methods for gaining insight and improving the thermal design of MV switchgear.

ACKNOWLEDGMENTS

The authors would like to thank the two master student groups at TUC who performed the preliminary tests and simulations during their fall project 2014.

REFERENCES

[1] T.R. Bjørtuft et al., 2013, "Dielectric and thermal challenges for next generation ring main units (RMU)", *Proceedings CIRED conference*, Stockholm, Paper 0463.

[2] IEC 62271-1:2011 ed. 1.1, High-voltage switchgear and controlgear - Part 1: Common specifications.

[3] IEC/TR 60890:2014 ed. 2.0, A method of temperature-rise verification of low-voltage switchgear and controlgear assemblies by calculation.

[4] Switchgear Manual, 6th edition, 1978, Brown, Boveri & CIE Aktiengesellschaft, Mannheim, Germany.

[5] R. Holm, 1967, *Electric Contacts. Theory and Applications*, Springer-Verlag, Berlin, Germany.

[6] M. Braunovic, 1999, Power Connections. In: P.G. Slade, *Electrical Contacts*, Taylor & Francis Group, Boca Raton, USA, pp. 222-223.

[7] X. Dong et al., 2009, "Thermal network analysis in MV GIS design", *Proceedings CIRED conference*, Prague, Paper 0637.